nature climate change

LETTERS

PUBLISHED ONLINE: 2 SEPTEMBER 2012 | DOI: 10.1038/NCLIMATE1682

Robust projections of combined humidity and temperature extremes

E. M. Fischer* and R. Knutti

Impacts of climate change such as the effects on human discomfort, morbidity and mortality often depend on multiple climate variables. Thus, a comprehensive impact assessment is challenging and uncertainties in all contributing variables need to be taken into account. Here we show that uncertainties in some impact-relevant metrics such as extremes of health indicators are substantially smaller than generally anticipated. Models that project greater warming also show a stronger reduction in relative humidity. This joint behaviour of uncertainties is particularly pronounced in mid-continental land regions of the subtropics and mid-latitudes where the greatest changes in heat extremes are expected. The uncertainties in health-related metrics combining temperature and humidity are much smaller than if uncertainties in the two variables were independent. Such relationships also exist under present-day conditions where the effect of model biases in temperature and relative humidity largely cancel for combined quantities. Our results are consistent with thermodynamic first principles. More generally, the findings reveal a large potential for joint assessment of projection uncertainties in different variables used in impact studies.

During recent major summer heatwaves, such as in 2003 in central and western Europe and 2010 in Russia, the mortality locally increased by tens of thousands of additional casualties[1]. Apart from excessive temperature anomalies, other factors such as humidity, radiation, low winds and air pollution potentially contributed to the enhanced mortality and more generally to the human discomfort. Likewise, many other socio-economic or ecological climate impacts, for example on agricultural production, forest fires, glacier retreat, river runoff or energy production, depend on more than one climate variable. Consequently, for a comprehensive assessment of climate change impacts it is imperative to take into account the uncertainties in all contributing variables.

In many cases the different climate variables are linked through first principles or basic mechanisms that are well understood, for example, warmer air being able to hold more moisture, or soil moisture variations affecting the partitioning of sensible and latent heat. The relationships depend on the temporal resolution of the variables considered and may vary across different quantiles[2,3]. In many cases they have been found to be relatively well captured by models, for example, for temperature and precipitation[4,5]. Despite the knowledge about the relationships across variables, they are often ignored in the context of projections. The Fourth Assessment Report of the Intergovernmental Panel on Climate Change[6], for example, provides projections of many variables, but each of those is discussed separately. Recently some studies have quantified how relationships across variables evolve into the future[7,8] or how their often correlated uncertainties can be transformed into joint probabilistic projections[9,10]. However, there is a serious lack of research addressing joint projections in variables other than temperature and precipitation.

Here we use simulations from 15 general circulation models (GCMs; Supplementary Table S1) of the new Climate Model Intercomparison Project phase 5 (CMIP5; ref. 11) to demonstrate that in selected cases uncertainties in impact-relevant variables are smaller than generally anticipated. To this end, we focus on two variables that are considered as well-established risk factors for human health: temperature and humidity. High ambient temperatures and humidity reduce the human body's efficiency of transporting away the metabolic heat through evaporative cooling (sweating) and heat conduction[12]. Consequently, they lead to heat stress and can increase both morbidity and mortality[13]. To quantify the combined effects of temperature and humidity we here use the simplified wet-bulb globe temperature (W; refs 12,14,15) and the thermodynamically motivated equivalent temperature[16,17] (see Methods).

Figure 1 illustrates the 2 m temperatures and relative humidity on the 1% warmest days (hereafter, $T_{x1\%}$ and $\mathrm{RH}_{x1\%}$) of the period 1986–2005 for each GCM (red dots). In both Southern Australia (SAU) and Central North America (CNA), present-day $T_{x1\%}$ and $\mathrm{RH}_{x1\%}$ vary strongly across models (SAU, $T_{x1\%}$: 29–36 °C, $\mathrm{RH}_{x1\%}$: 17–46%; CNA, $T_{x1\%}$: 28–37 °C, $\mathrm{RH}_{x1\%}$: 24–59%). The corresponding values derived from the European Centre for Medium-Range Weather Forecasts (ECMWF) Reanalysis (ERA) Interim (Fig. 1, yellow dots) and National Centers for Environmental Prediction—Department of Energy (NCEP-DOE) Reanalysis 2 (Fig. 1, white dots; see Methods) fall within the range of GCMs. To illustrate the model spread we fit a kernel density estimate[18] to the bivariate distribution (Fig. 1, red shading). Given the limited number of models the kernel density should be interpreted with caution. However, it is evident that models showing hotter temperatures tend to simulate lower relative humidity. Despite the large spread in the contributing variables, models agree remarkably well on W on the hottest 1% of days ($W_{x1\%}$, solid black lines mark equal W levels) and the model spread in $W_{x1\%}$ is substantially smaller than if the inter-model differences in the two variables were uncorrelated (Fig. 1 grey shading). The reduction of model spread is even more pronounced for equivalent temperature (T_{eq}, that is, the temperature an air parcel would have if all water vapour were condensed; see Methods), which demonstrates that the result is consistent with thermodynamical first principles. The agreement between models and cancellation of model differences is a consequence of the negative correlation between $\mathrm{RH}_{x1\%}$ and $T_{x1\%}$. This negative correlation is limited mainly to mid-continental land regions in North America, Eurasia, the Amazonian basin and parts of Australia (Supplementary Fig. S1). In these regions the relationship implies that the pronounced differences in temperature

Institute for Atmospheric and Climate Science, ETH Zurich, Universitätstrasse 16, 8092 Zurich, Switzerland. *e-mail: erich.fischer@env.ethz.ch.

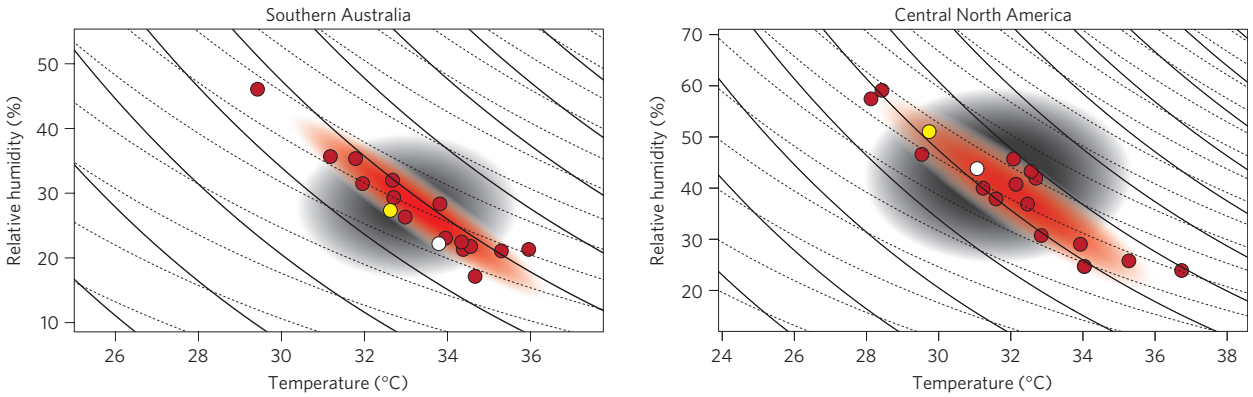

Figure 1 | Model agreement in maximum heat stress. Relative humidity ($RH_{x1\%}$) versus temperature ($T_{x1\%}$) averaged across the hottest 1% of days (defined as all days exceeding the local 99th percentile of daily temperatures) of the period 1986–2005 (historical simulation with all forcings). Variables are averaged across SAU (110°–155° E and 30°–45° S) and CNA (85°–103° W and 30°–50° N). The red points mark individual CMIP5 models and the red shading illustrates the joint uncertainty spanned by the model range. The grey-to-black shading illustrates the corresponding range if $T_{x1\%}$ and $RH_{x1\%}$ were uncorrelated. The yellow and white points show the reanalysis data for ERA Interim and NCEP-DOE Reanalysis 2, respectively, for the period 1986–2005. The black solid lines mark isolines of equal equivalent temperatures (T_{eq}) and the dashed lines mark isolines of equal simplified wet-bulb globe temperatures (W).

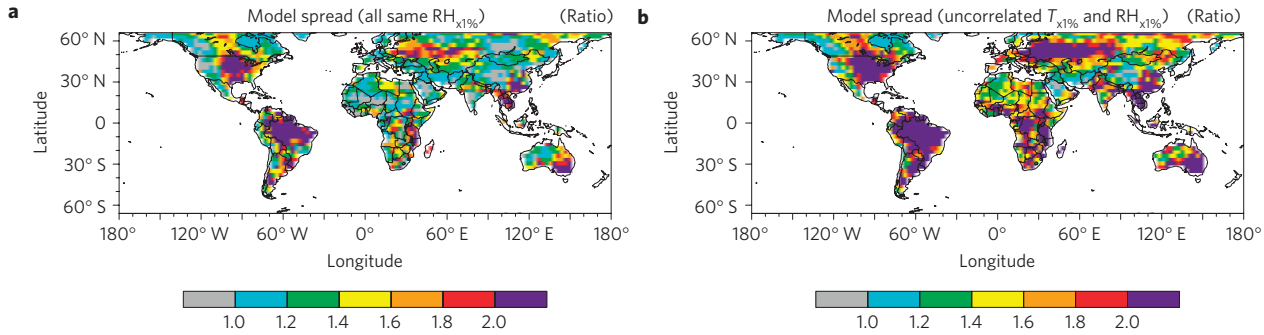

Figure 2 | Reduction in model spread resulting from temperature and humidity correlation. The panels show the ratio of potential versus actual model spread (2σ across all 15 GCMs) in simplified wet-bulb globe temperatures during hottest 1% of days ($W_{x1\%}$). **a**, The ratio by which model spread would be larger if all models had the same $RH_{x1\%}$ (ensemble mean calculated for each grid box; ratio 2 indicates that model spread would be twice of what it actually is). **b**, The ratio by which model spread was larger if $T_{x1\%}$ and relative $RH_{x1\%}$ were completely uncorrelated and their spread was considered fully independent.

and humidity across models tend to cancel in terms of atmospheric heat content, expressed as T_{eq}. Consequently, the biases in $W_{x1\%}$ (Supplementary Fig. S2) and $T_{eqx1\%}$ (Supplementary Fig. S3) with respect to the reanalyses are substantially smaller than expected from the biases in $T_{x1\%}$ and $RH_{x1\%}$. These findings demonstrate that despite model deficiencies in characteristics of, for example, convective precipitation, soil hydrology and cloud formation that potentially contribute to the considerable regional biases in hot extremes ($T_{x1\%}$), the GCM ensemble mean generally agrees well with $W_{x1\%}$ and $T_{eqx1\%}$ in reanalysis data, particularly over CNA and SAU.

Figure 2 shows the cancellation of the model spread resulting from the correlation of temperature and humidity. The spread in $W_{x1\%}$ across models (expressed as 2σ) would be substantially greater if $RH_{x1\%}$ at a given grid point was the same in all models, that is, if the higher temperatures were not compensated by humidity deficits (Fig. 2a). If the contributing variables were completely independent, the spread in $W_{x1\%}$ would be more than doubled in many regions if $T_{x1\%}$ and $RH_{x1\%}$ (Fig. 2b). This is further illustrated by the grey shading in Fig. 1 combining the spread in $T_{x1\%}$ and $RH_{x1\%}$ as if they were unrelated. Negative correlations are also found if relative humidity and temperature on the 5% or 10% warmest days are considered instead of the hottest 1% of days. The relation weakens towards lower quantiles but is still significant for summer means.

We find a similar joint behaviour of temperature and humidity under climate change, that is, models that simulate stronger warming also tend to show stronger $RH_{x1\%}$ reduction, shown in Fig. 3. The correlation between warming and drying is robust across different representative concentration pathways (RCP4.5 and RCP8.5) in CMIP5 and the emission scenario A1B in CMIP3. However, the relation across models, which is here illustrated for western North America, CNA and southern Europe and the Mediterranean is limited to roughly the same regions that exhibit a pronounced negative correlation under present-day conditions (Supplementary Fig. S4). Those regions, in particular the northern subtropics to mid-latitudes, can be considered as hotspots because they experience the largest ensemble mean change in $T_{x1\%}$ (Fig. 3a) and thus, the greatest reduction in return periods of hot extremes[19,20]. In those regions, the warming and drying signals involve very large model uncertainties, as shown for temperature in Fig. 4b. Given those uncertainties in changes of temperature and humidity, one would expect projections of the combined impact-relevant variable $W_{x1\%}$ to be of little value. However, owing to the correlation in the change of the two contributing variables (Fig. 3), the resulting uncertainty in the projections of the maximum heat stress $W_{x1\%}$ is surprisingly low.

Across many land regions the uncertainty range in $W_{x1\%}$ (Fig. 4d) is no greater or even smaller (particularly in the hotspot

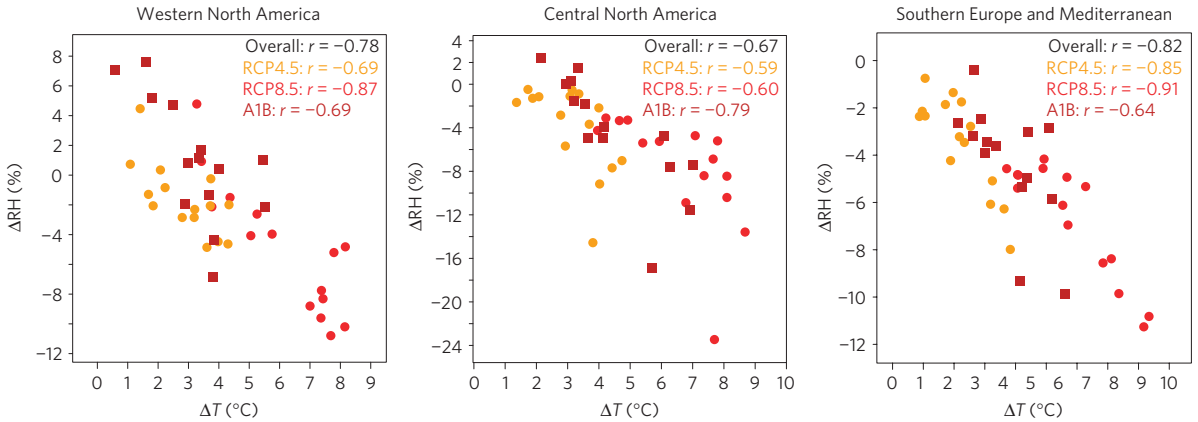

Figure 3 | Joint projections in hot extremes and humidity. Change in regional average temperature and relative humidity on the hottest 1% of days ($T_{x1\%}$ and $RH_{x1\%}$) averaged across the three regions western North America (103°–130° W and 30°–60° N), CNA (85°–103° W and 30°–50° N), Southern Europe and the Mediterranean (10° W–40° E and 30°–48° N). The circles mark the 15 GCMs of the CMIP5 experiment (red for RCP8.5, orange for RCP4.5) and the brown squares mark the 14 GCMs from the CMIP3 experiment (for A1B scenario). Changes are shown for the period 2081–2100 relative to 1986–2005 for the CMIP5 models and relative to 1981–2000 for the CMIP3 models. 2 m temperatures and relative humidity are shown for CMIP5, whereas for CMIP3 the values are shown at the 925 hPa level owing to a lack of daily model output at surface levels.

regions) than the corresponding uncertainty in $T_{x1\%}$ (Fig. 4b). The uncertainty in $W_{x1\%}$ would be substantially larger if the $RH_{x1\%}$ change was assumed to be identical in all models (Fig. 4e). If $T_{x1\%}$ and $RH_{x1\%}$ changes were uncorrelated across models the uncertainties in $W_{x1\%}$ would be locally larger by a factor of two or more in many land regions (Fig. 4f). Only over dry desert regions such as the Sahara or Namib Desert the uncertainties in $T_{x1\%}$ and $RH_{x1\%}$ do not tend to offset each other.

We argue that the above joint behaviour arises from simple physical processes. On global scales and over open water bodies, near-surface humidity of the air roughly follows the increasing temperatures according to the Clausius–Clapeyron relationship, and thus relative humidity remains roughly constant[21]. This is not necessarily the case over land, where evapotranspiration may be limited, and models thus project decreasing $RH_{x1\%}$ particularly during the hottest days of the year. This behaviour arises from a lack of soil moisture that reduces latent and enhances sensible heat flux and thereby amplifies temperature extremes and at the same time dries the planetary boundary layer. Consequently, the partitioning of the heat content of the near-surface air into enthalpy and latent heat differs across models, whereas their sum, the atmospheric heat content H is robust. This explanation is supported by the good agreement among model projections for T_{eq}.

The above mechanism is further supported by the spatial patterns in the $T_{x1\%}$ and $RH_{x1\%}$ signal. The areas showing the greatest warming of the hottest 1% of days also experience the strongest $RH_{x1\%}$ reduction (Supplementary Fig. S5). The pattern correlation is highly significant for all but one model ($r < -0.6$ in 7 GCMs), and for the model average ($r = -0.76$). As a result, the climate change signal in $W_{x1\%}$ is more uniform (Fig. 4c) than the heterogeneous pattern of $T_{x1\%}$ (ref. 14). The greatest warming in dry regions (becoming even drier) and the weakest warming in humid regions (remaining humid, for example, tropical Africa and southeast Asia) tend to yield the same response of W owing to the nonlinearity in its definition and thus result in a spatially homogeneous $W_{x1\%}$ response pattern. Consistent with earlier studies, heat stress is projected to increase over all land regions along with rising temperatures. Using the concept of equivalent temperature, the changes in heat stress ($\Delta T_{eqx1\%}$) can be separated into a relative contribution from temperature ($\Delta T_{x1\%}$) and from humidity content (L_v/C_p) $\Delta q_{x1\%}$ (ref. 22) The change in temperature alone explains 60–80% of the change in equivalent temperature over the dry mid-latitudes. However, along the coasts and over the humid regions such as the tropics and southeast Asia roughly two-thirds of the change in $T_{eqx1\%}$ would be missed if the change in specific humidity was neglected. This supports earlier findings that the humidity-induced heat stress amplification is strongest in the regions that are warmest and most humid under present-day conditions[14,23,24].

The above examples highlight two remarkable findings that have broader implications: models agree remarkably well on a highly challenging measure such as present-day extremes of heat stress indicators and the uncertainties in the projection of these indicators are much smaller than expected from the uncertainties in the contributing variables. More generally, the first finding highlights that joint variability should be considered in the evaluation of present-day model performance. We provide a prominent example for covariability in model biases, which may exist in numerous other sets of variables. The fact that models tend to agree on variables such as equivalent temperature that have been highlighted as key metrics for the assessment of climate change[16] should increase our confidence in those models. On the other hand, our findings also demonstrate that certain simulated variables may agree with observations for the wrong reasons and thus are not ideal for model evaluation. Another consequence is that model biases in one variable affect biases in other variables. Nevertheless, a common assumption made in climate projections is that model biases from control integrations can be subtracted (the so-called constant-bias approach). Our results confirm that for certain variables this may be problematic, as pointed out earlier for temperature extremes in Europe[25].

The second finding underlines that there is a need to develop frameworks for joint uncertainty projections, rather than focusing on uncertainties in individual variables alone. Thereby, the relevant impacts should be taken into account when discussing the joint probability. If, for instance, the multi-model ensemble were used to estimate the risk of fire weather, conclusions would be opposite. Low humidity and high temperatures are well established risk factors for wild fires[26] among many other factors. Consequently, for such an impact variable the uncertainties in humidity and temperature would add up rather than compensate, giving rise to very large uncertainties in fire weather indices. Our results underline the need for statistical frameworks for a quantitative multivariate assessment. They could complement existing approaches of combining model averages in model variables as best estimates, even though these may not represent

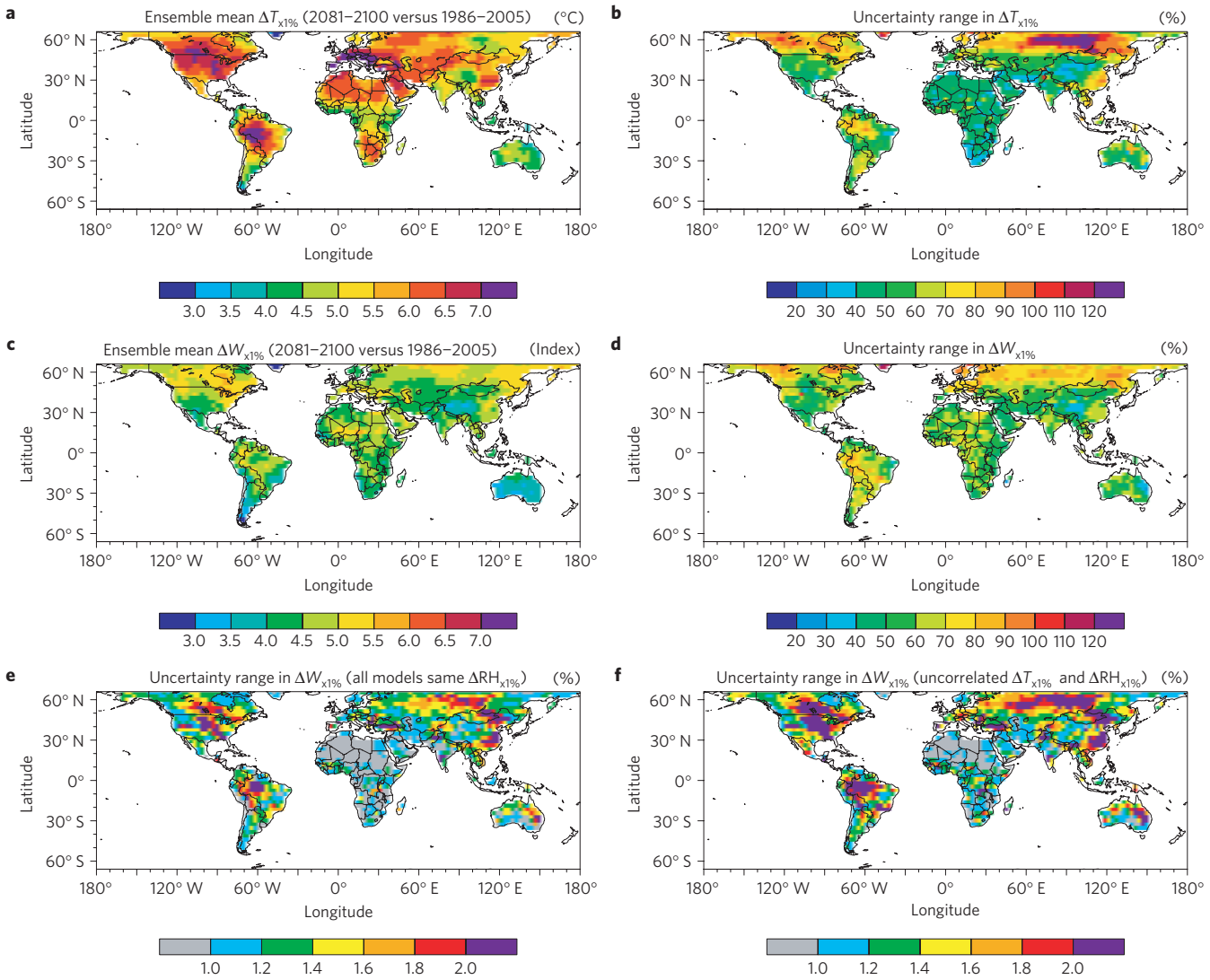

Figure 4 | Reduction of uncertainty in joint projections. a,**b**, Ensemble mean change in $T_{x1\%}$ (**a**) for RCP8.5 in 2081–2100 with respect to 1986–2005 and corresponding uncertainties (**b**). Uncertainties are expressed as 2σ across the changes in 15 GCMs of the CMIP5 experiment relative to the mean change, expressed as a percentage. **c**,**d**, The same as **a**,**b** but for change in $W_{1x\%}$, the simplified wet-bulb globe temperatures on the hottest 1% of days. **e**,**f**, Ratio by which the uncertainties in **d** would be larger/smaller if the change in $RH_{x1\%}$ were the same in all models (that is, local ensemble mean change). **f** is the same as in **e** but if the change in $T_{x1\%}$ and $RH_{x1\%}$ were independent.

plausible model states[27] and may not correspond to the joint best estimate in a multivariate sense.

We see great potential in studying other sets of variables such as the difference of precipitation and evapotranspiration (P–E), a relevant measure for large-scale hydrology and agriculture that is expected to be better constrained than the individual variables P and E. Ultimately, such multivariate considerations are vital for impact assessments that allow stake-holders to take well-informed decisions on adaptation strategies.

Methods

The simplified wet-bulb globe temperature[12,14,15] (W) is defined as $W = 0.567T + 0.393e + 3.94$, where T is the temperature in degrees Celsius and e is the simultaneous vapour pressure in hectopascals. Here, it is calculated at each grid box on the basis of daily mean temperatures and mean vapour pressure. In Fig. 1 W on the hottest 1% of days ($W_{x1\%}$) for each pair of variables is calculated on the basis of the saturation vapour pressure e_{sat} derived from T and relative humidity.

The findings are consistent with the thermodynamical concept of the atmospheric heat content, $H = C_p T + L_v q$, (also referred to as moist static energy or moist enthalpy)[28], where C_p is the specific heat of air at constant pressure ($\sim$1,005 J kg^{-1} K^{-1}), T is the temperature, L_v is the latent heat of vaporization ($\sim 2.430 \times 10^6$ J kg^{-1} at 30 °C) and q is the specific humidity. To compare the model behaviour in a thermodynamically motivated metric, we calculate the equivalent temperature $T_{eq} = H/C_p = T + (L_v q)/C_p$. T_{eq} is similar to T during cold winter days but can differ strongly during warm and particularly humid winter days.

The model results for present-day conditions are compared against daily output at surface levels of reanalyses data for the same period (1986–2005) from the ECMWF ERA Interim reanalysis[29] and the NCEP-DOE Reanalysis 2 (ref. 30). The data are processed at the native grid and the final fields are regridded for comparison with the model products.

Received 6 June 2012; accepted 8 August 2012; published online 2 September 2012

References

1. Barriopedro, D., Fischer, E. M., Luterbacher, J., Trigo, R. & Garcia-Herrera, R. The hot summer of 2010: Redrawing the temperature record map of Europe. *Science* **332,** 220–224 (2011).
2. Hirschi, M. *et al.* Observational evidence for soil-moisture impact on hot extremes in southeastern Europe. *Nature Geosci.* **4,** 17–21 (2011).
3. Gallant, A. J. E. & Karoly, D. J. A combined climate extremes index for the Australian region. *J. Clim.* **23,** 6153–6165 (2010).
4. Trenberth, K. E. & Shea, D. J. Relationships between precipitation and surface temperature. *Geophys. Res. Lett.* **32,** L14703 (2005).

5. Adler, R. F. *et al.* Relationships between global precipitation and surface temperature on interannual and longer timescales (1979–2006). *J. Geophys. Res.* **113,** D22104 (2008).
6. Meehl, G. A. *et al.* in *IPCC Climate Change 2007: The Physical Science Basis* (eds Solomon, S. *et al.*) 747–846 (Cambridge Univ. Press, 2007).
7. Beniston, M. Trends in joint quantiles of temperature and precipitation in Europe since 1901 and projected for 2100. *Geophys. Res. Lett.* **37,** L07707 (2009).
8. Vidale, P. L., Luthi, D., Wegmann, R. & Schar, C. European summer climate variability in a heterogeneous multi-model ensemble. *Climatic Change* **81,** 209–232 (2007).
9. Watterson, I. M. Calculation of joint PDFs for climate change with properties matching Australian projections. *Aust. Meteorol. Oceanogr. J.* **61,** 211–219 (2011).
10. Tebaldi, C. & Sanso, B. Joint projections of temperature and precipitation change from multiple climate models: A hierarchical Bayesian approach. *J. R. Stat. Soc. Ser. A* **172,** 83–106 (2009).
11. Taylor, K. E., Stouffer, R. J. & Meehl, G. A. A summary of the CMIP5 experiment design. *Bull. Am. Meteorol. Soc.* **93,** 485–498 (2012).
12. Sherwood, S. C. & Huber, M. An adaptability limit to climate change due to heat stress. *Proc. Natl Acad. Sci. USA* **107,** 9552–9555 (2010).
13. Basu, R. & Samet, J. M. Relation between elevated ambient temperature and mortality: a review of the epidemiological evidence. *Epidemiol. Rev.* **24,** 190–202 (2002).
14. Fischer, E. M., Oleson, K. W. & Lawrence, D. M. Contrasting urban and rural heat stress responses to climate change. *Geophys. Res. Lett.* **39,** L03705 (2012).
15. Willett, K. M. & Sherwood, S. Exceedance of heat index thresholds for 15 regions under a warming climate using the wet-bulb globe temperature. *Int. J. Climatol.* **32,** 161–177 (2012).
16. Pielke, R. A. Heat storage within the earth system. *Bull. Am. Meteorolo. Soc.* **84,** 331–335 (2003).
17. Fall, S., Diffenbaugh, N. S., Niyogi, D., Pielke, R. A. Sr & Rochon, G. Temperature and equivalent temperature over the United States (1979–2005). *Int. J. Climatol.* **30,** 2045–2054 (2010).
18. Duong, T. Kernel density estimation and kernel discriminant analysis for multivariate data in R. *J. Stat. Softw.* **21,** 1–16 (2007).
19. Kharin, V. V., Zwiers, F. W., Zhang, X. B. & Hegerl, G. C. Changes in temperature and precipitation extremes in the IPCC ensemble of global coupled model simulations. *J. Clim.* **20,** 1419–1444 (2007).
20. Orlowsky, B. & Seneviratne, S. I. Global changes in extreme events: Regional and seasonal dimension. *Climatic Change* **110,** 669–696 (2012).
21. Sherwood, S. C. *et al.* Relative humidity changes in a warmer climate. *J. Geophys. Res.* **115,** D09104 (2010).
22. Pielke, R. A., Morgan, J. & Davey, C. Assessing 'global warming' with surface heat content. *Eos* **85,** 210–211 (2004).
23. Delworth, T., Mahlman, J. & Knutson, T. Changes in heat index associated with CO_2-induced global warming. *Climatic Change* **43,** 369–386 (1999).
24. Fischer, E. M. & Schär, C. Consistent geographical patterns of changes in high-impact European heatwaves. *Nature Geosci.* **3,** 398–403 (2010).
25. Boberg, F. & Christensen, J. H. Overestimation of Mediterranean summer temperature projections due to model deficiencies. *Nature Clim. Change* **2,** 433–436 (2012).
26. Dale, V. H. *et al.* Climate change and forest disturbances. *Bioscience* **51,** 723–734 (2001).
27. Knutti, R., Furrer, R., Tebaldi, C., Cermak, J. & Meehl, G. Challenges in combining projections from multiple climate models. *J. Clim.* **23,** 2739–2758 (2010).
28. Peterson, T. C., Willett, K. M. & Thorne, P. W. Observed changes in surface atmospheric energy over land. *Geophys. Res. Lett.* **38** (2011).
29. Dee, D. P. *et al.* The ERA-Interim reanalysis: Configuration and performance of the data assimilation system. *Quart. J. Roy. Meteorol. Soc.* **137,** 553–597 (2011).
30. Kanamitsu, M. *et al.* NCEP-DOE AMIP-II reanalysis (R-2). *Bull. Am. Meteorol. Soc.* **83,** 1631–1643 (2002).

Acknowledgements

This research was supported by the Swiss National Science Foundation (NCCR Climate).

Author contributions

E.M.F. performed the analysis of the models. Both authors contributed extensively to the idea and the writing of this paper.

Additional information

Supplementary information is available in the online version of the paper. Reprints and permissions information is available online at www.nature.com/reprints. Correspondence and requests for materials should be addressed to E.M.F.

Competing financial interests

The authors declare no competing financial interests.